Turbulence Structure and Mixing Intensity in Stably Stratified Boundary-Layer Flows over Thermally Heterogeneous Surfaces

Dmitrii Mironov(1) *and Peter Sullivan*(2)

(1) German Weather Service, Offenbach am Main, Germany

(2) National Center for Atmospheric Research, Boulder, CO, USA

(dmitrii.mironov@dwd.de, pps@ucar.edu)

Outline

- Motivation
- Flow governing parameters
- Simulation set-up, DNS data set
- Results: mean fields, variances and fluxes, skewness, flow visualization, third-order transport of temperature variance
- Implications for SBL parameterization
- Work in progress and outlook

Motivation

- Poor understanding of the role of horizontal thermal heterogeneity in maintaining turbulent fluxes

- Most parameterization schemes of stably stratified PBL, incl. surface layer, do not account for many important features (e.g., gravity waves, meanders of cold air, radiation flux divergence, and horizontal thermal heterogeneity of the underlying surface)

Motivation (cont'd)

- Atmospheric models (e.g., NWP models) typically underestimate SBL mixing
- Models tend to quench turbulence in strongly stable stratification
- Ad hoc tuning devices like "minimum diffusion coefficients" do not help much, they are often detrimental for the NWP/climate model performance (e.g., by making SBL too diffusive)

Motivation (cont'd)

- Although most turbulence models are based on truncated second-moment budget equations, little attention has been paid to the second-moment budgets in stably stratified PBLs (cf. Mason and Derbyshire 1990, Coleman et al. 1992, Andrén 1995, Kosović and Curry 2000, Saiki et al. 2000, Jiménez and Cuxart 2005, Taylor and Sarkar 2008, Ansorge 2011, Heinze at al. 2015, Shah and Bou-Zeid 2014)

LES of Weakly Stable PBL

(Mironov and Sullivan 2016, *J. Atmos. Sci.*, **73**, 449-464.)

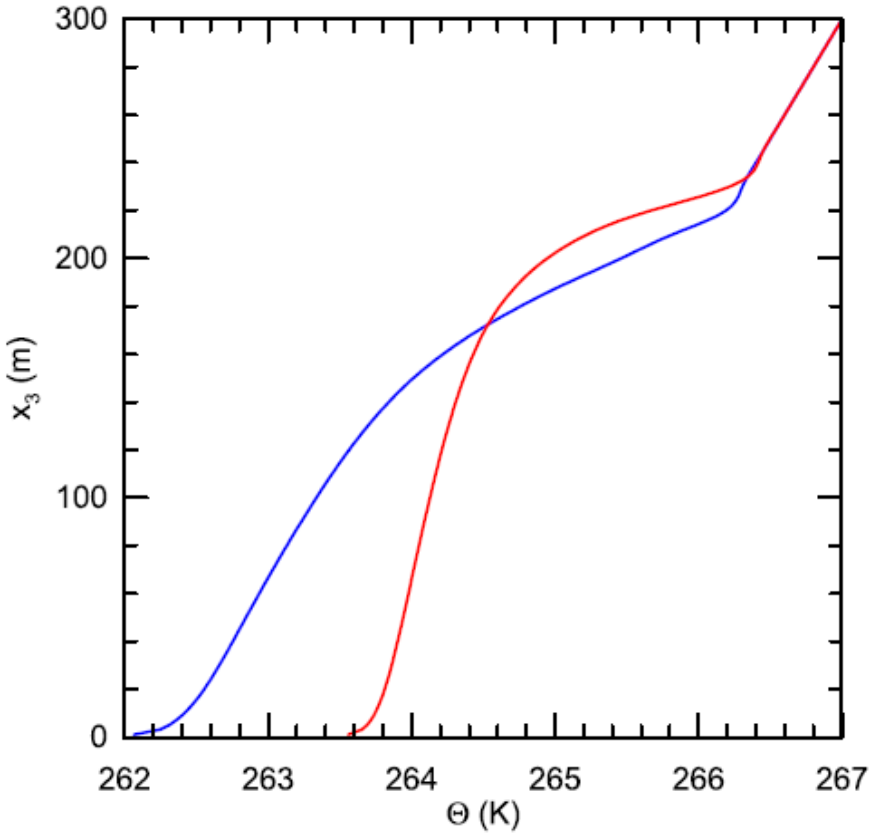

Mean temperature from simulations HOM (blue) and HET (red).

- The SBL over a heterogeneous surface (HET) has larger TKE and is better vertically mixed as compared to its homogeneous counterpart (HOM).
- The temperature variance plays a key role in enhanced mixing; the increase in $<\theta'^2>$ near the heterogeneous surface explains the reduced magnitude of the downward buoyancy flux and the ensuing increase in TKE that leads to more vigorous mixing.
- Because of surface heterogeneity, the turbulent transport term (divergence of the third-order moment) in the $<\theta'^2>$ budget not only redistributes the temperature variance vertically but is a net gain.

Important point. The SBL in both HOM and HET is turbulent (weakly-to-moderately stable regime!).

Strongly Stable PBL

Key questions

- If turbulence dies out over a homogeneous surface due to strong static stability (cf. weakly stable regime), would it survive over a heterogeneous surface?
- If so, how anisotropic turbulence is, and does it generate appreciable vertical fluxes of momentum and scalars?
- How turbulence anisotropy and fluxes of momentum and scalars in strongly stable regimes can be parameterized in NWP and climate models?

LESs of strongly stable flows are uncertain because of the SGS parameterizations, DNS is more appropriate.

Couette Flow Configuration

- The fluid depth is H.
- The lower boundary is at rest.
- The upper boundary moves with a constant velocity U_u.
- Stable buoyancy stratification is maintained by a (constant) temperature difference $\Delta\theta = \theta_u - \theta_l$ between the upper and lower boundaries.
- The temperature at the horizontal upper and lower surfaces is either homogeneous or **varies sinusoidally in the streamwise direction**, while **the horizontal-mean temperature is the same in the homogeneous and heterogeneous cases**.

Governing Equations

The length H, velocity U_u, time H/U_u and temperature $\Delta\theta$ scales are used to make the problem dimensionless.

Governing equations (in dimensionless form):

$$\left(\frac{\partial}{\partial t}+u_k\frac{\partial}{\partial x_k}\right)u_i=-\frac{\partial p}{\partial x_i}+\delta_{i3}\mathrm{Ri}\,\theta+\frac{1}{\mathrm{Re}}\frac{\partial^2 u_i}{\partial x_k^2},$$

$$\frac{\partial u_i}{\partial x_i}=0,$$

$$\left(\frac{\partial}{\partial t}+u_k\frac{\partial}{\partial x_k}\right)\theta=\frac{1}{\mathrm{PrRe}}\frac{\partial^2\theta}{\partial x_k^2}.$$

Dimensionless parameters

$$\mathrm{Pr}=\frac{\nu}{\chi},\quad \mathrm{Re}=\frac{U_u H}{\nu},\quad \mathrm{Ri}=\frac{Hg\alpha_T\Delta\theta}{U_u^2}$$

Boundary Conditions

Periodic boundary conditions in the streamwise x_1 and the spanwise x_2 horizontal directions. At the horizontal boundaries

$$u_1 = 0, \quad u_2 = u_3 = 0, \quad \text{at} \quad x_3 = 0,$$
$$u_1 = 1, \quad u_2 = u_3 = 0, \quad \text{at} \quad x_3 = 1,$$

and

$$\theta = \delta\theta \sin\left[2\pi n x_1 / L_1\right] \quad \text{at} \quad x_3 = 0,$$
$$\theta = 1 + \delta\theta \sin\left[2\pi n \left(x_1 - U_u t\right) / L_1\right] \quad \text{at} \quad x_3 = 1,$$

where L_1 is the domain size in the x_1 direction, $\delta\theta$ is the (dimensionless) amplitude of the temperature variations at the upper and lower surfaces, and n is the number of cold and warm stripes (the number of surface temperature waves).

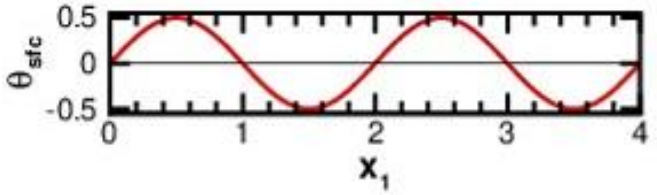

Governing Parameters of Simulated Cases

In all simulated cases, **Pr=1**, **Re=10^4**, **Ri=0.25**, **n=4**,
the domain size is **8**, **8** and **1**, and the number of grid points is **512**, **512** and **256**, in x_1, x_2 and x_3, directions, respectively.

Case	$\delta\theta$	T_t	T_s	Re_τ	$u_*\times10^2$	$Q_*\times10^5$	$1/L$
HOM	**0**	1115	15	104.63	1.05	–10.93	9.54
HET025	**0.25**	1166	166	100.50	1.01	–9.80	9.65
HET050	**0.50**	1392	392	107.77	1.08	–7.45	5.95
HET075	**0.75**	1380	380	112.16	1.12	–5.12	3.63

Here, T_t is the total length of the simulation (in dimensionless time units), T_s is the length of the sampling period (at the end of the run), u_* is the surface friction velocity, $u_*=\mathrm{Re}^{-1}\mathrm{Re}_\tau$ is the Reynolds number based on u_*, Q_* is the surface temperature flux, and L is the Obukhov length.

Spin-Up of Simulations

The homogeneous simulation starts with a fully developed, stationary, neutral Couette flow. The stable buoyancy stratification is established by gradually (linearly in time) increasing the Richardson number over 100 dimensionless time units from Ri=0 to Ri=0.25. The simulations are then continued until turbulence dies out and the laminar Couette flow regime is achieved. We give turbulence all the chances to survive, but **Ri=0.25 is sufficient to fully quench turbulence in the homogeneous case.**

The heterogeneous simulations start with Ri=0, $\delta\theta$=0, and the linear velocity and temperature profiles. The Richardson number is increased from Ri=0 to Ri=0.25 over 10 time units, while the temperature difference $\delta\theta$ is increased (linearly in time) from zero to its final value (see Table) over 100 time units. In order to assist initial turbulence spin-up, velocity and temperature fluctuations taken from the neutral turbulent Couette flow are added in the lower 1/4 and the upper 1/4 of the computational domain (**we give turbulence only a very little help**). The simulations are then continued over many time units required to achieve a quasi-stationary flow regime over heterogeneous surfaces, and then continued further in the quasi-stationary regime over the sampling period.

Resolution Issues

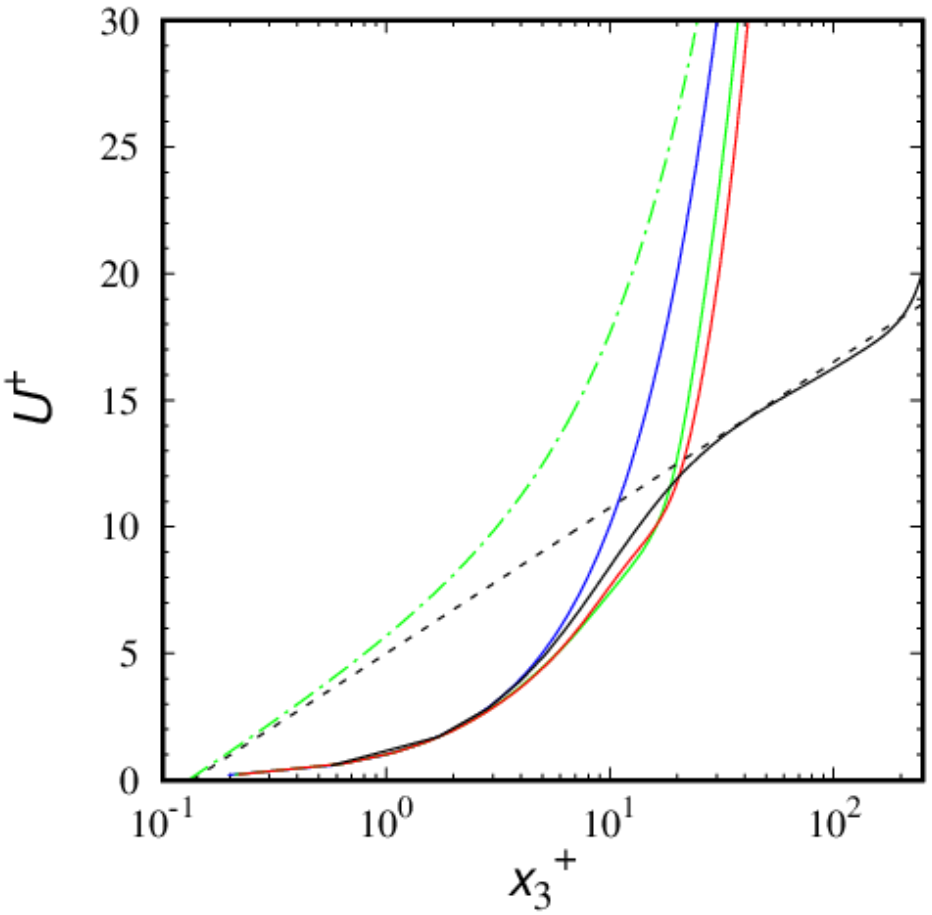

Dimensionless mesh size

$x_3^+ = u_* \Delta x_3 / \nu$

Just above the surface
$x_3^+ = 1$ is excellent,
$x_3^+ = 2$ (or somewhat larger) is usually sufficient.

In our configuration,
$x_3^+ < 0.3$ is required!

Streamwise mean-velocity component from simulations HET025 (blue), HET050 (green), and HET075 (red) plotted in wall units. **Black dashed** line shows the logarithmic velocity profile from neutral simulation, and **green dot-dashed** line shows the Monin-Obukhov log-linear velocity profile computed with u_* and Q_* from the simulation HET050.

Mean Fields

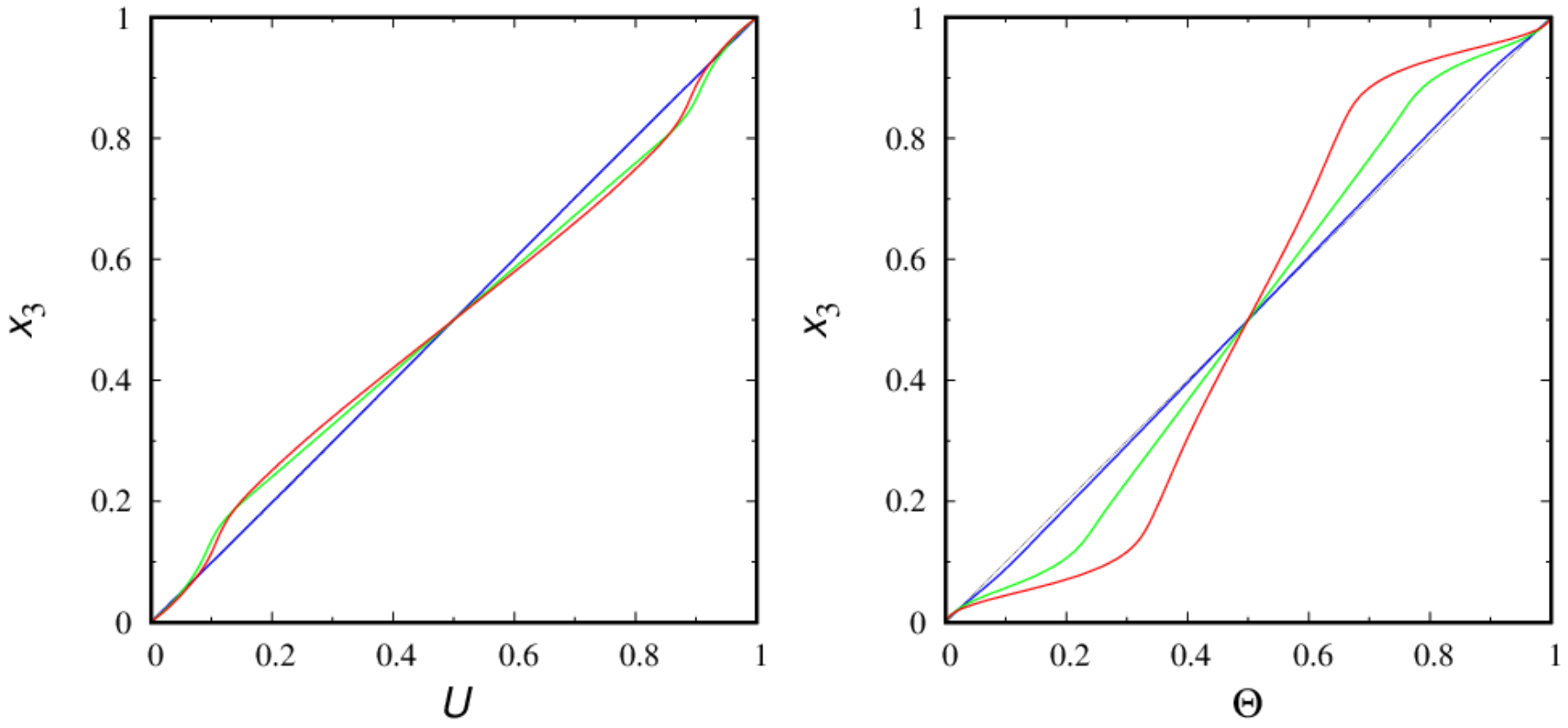

(**left**) Streamwise component of mean velocity, and (**right**) mean temperature from simulations HET025 (blue), HET050 (green), and HET075 (red). Thin black dotted line shows the laminar solution.

Stability Parameters

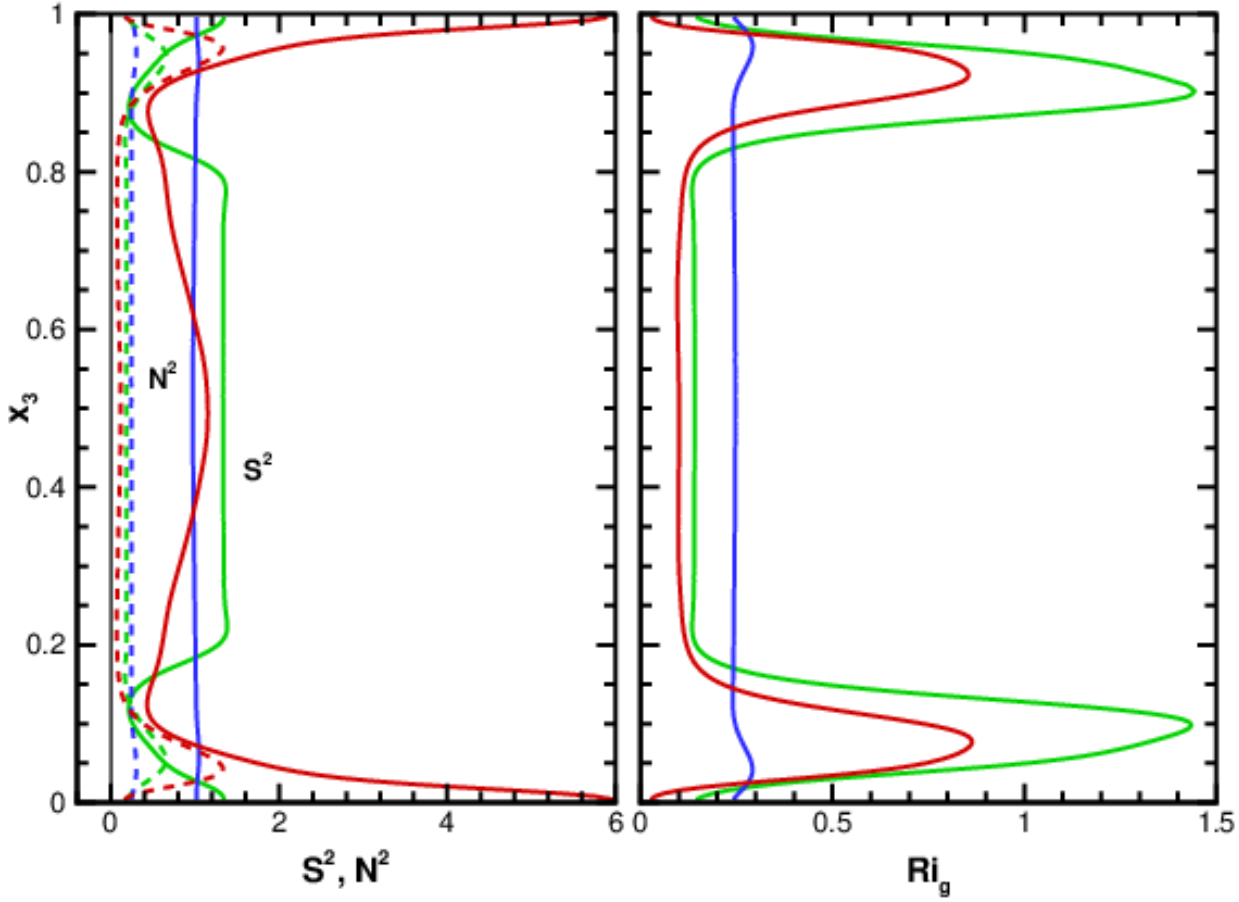

Vertical profiles of (shear, buoyancy) frequencies (S^2, N^2) denoted by (solid, dotted) lines, respectively (left panel), and gradient Richardson number Ri_g (right panel) for the heterogeneous simulations HET025 (blue), HET050 (green), and HET075 (red).

TKE

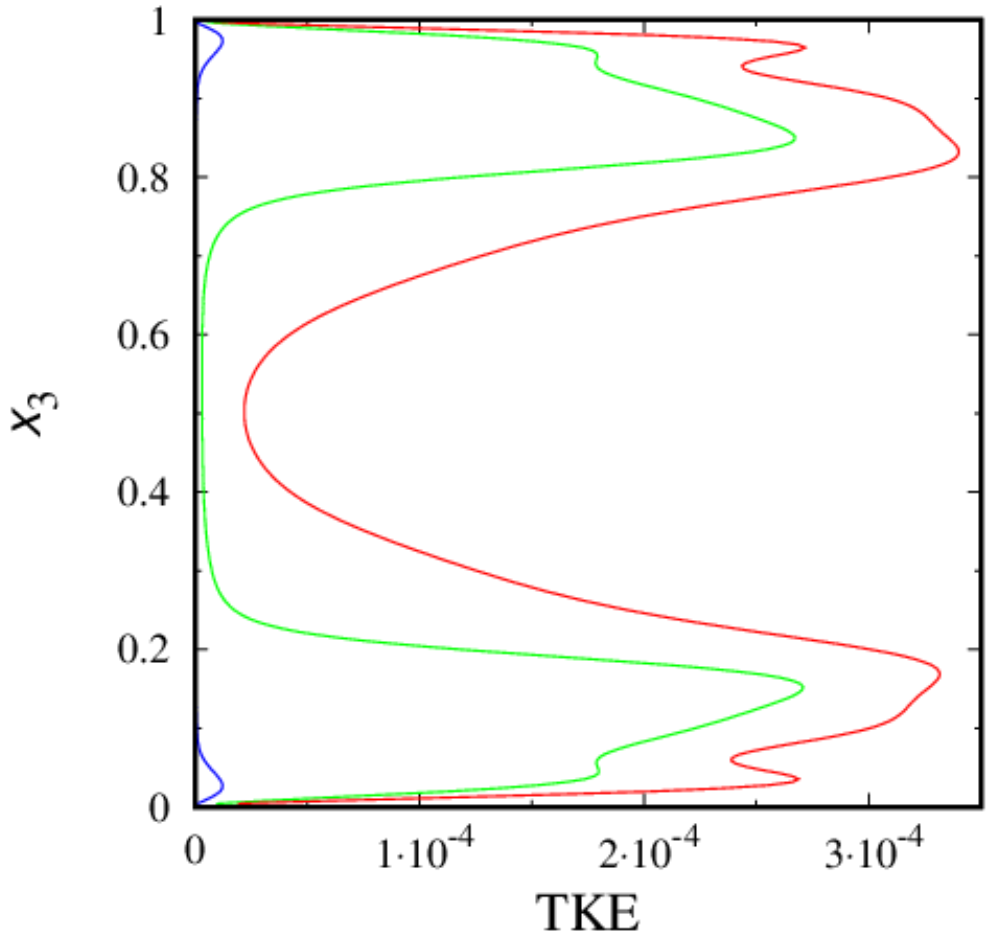

Turbulence kinetic energy from simulations HET025 (blue), HET050 (green), and HET075 (red).

Velocity Variances

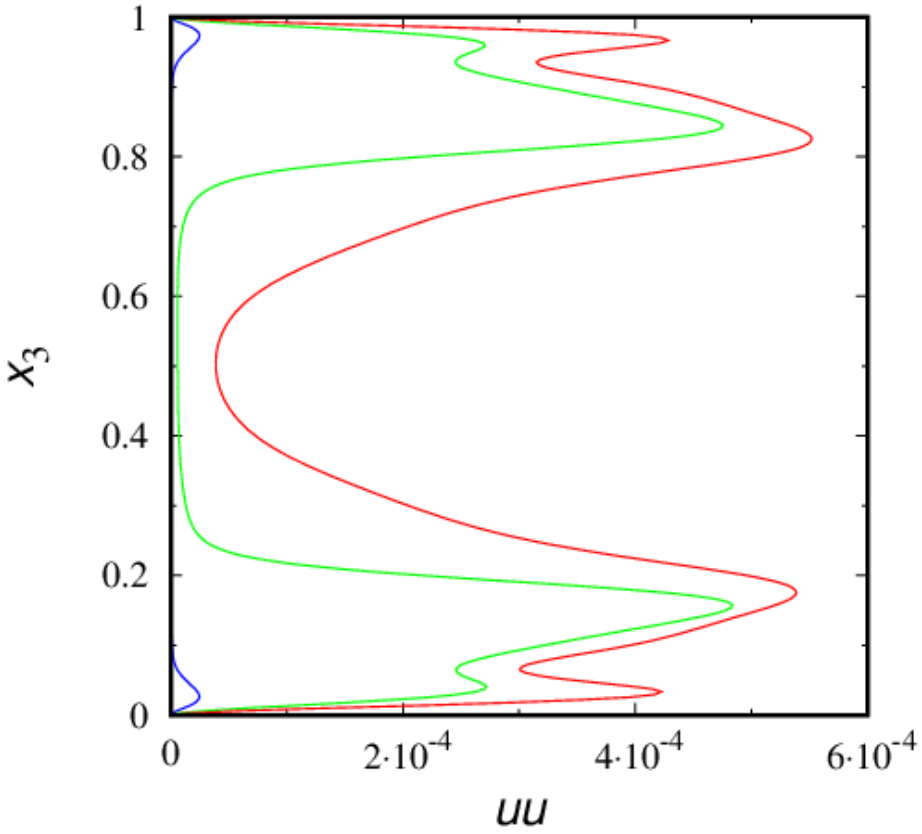

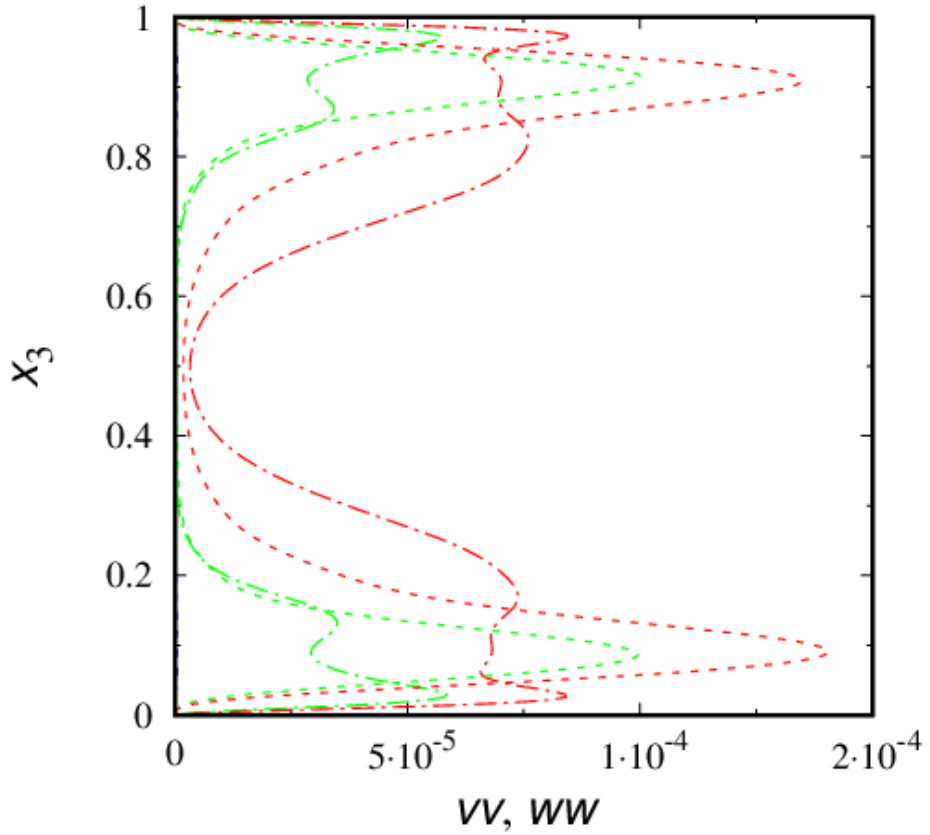

(**left**) Streamwise velocity variance, and (**right**) spanwise (dot-dashed curves) and vertical (dashed curves) velocity variances from simulations HET025 (blue), HET050 (green), and HET075 (red).

Turbulence Anisotropy

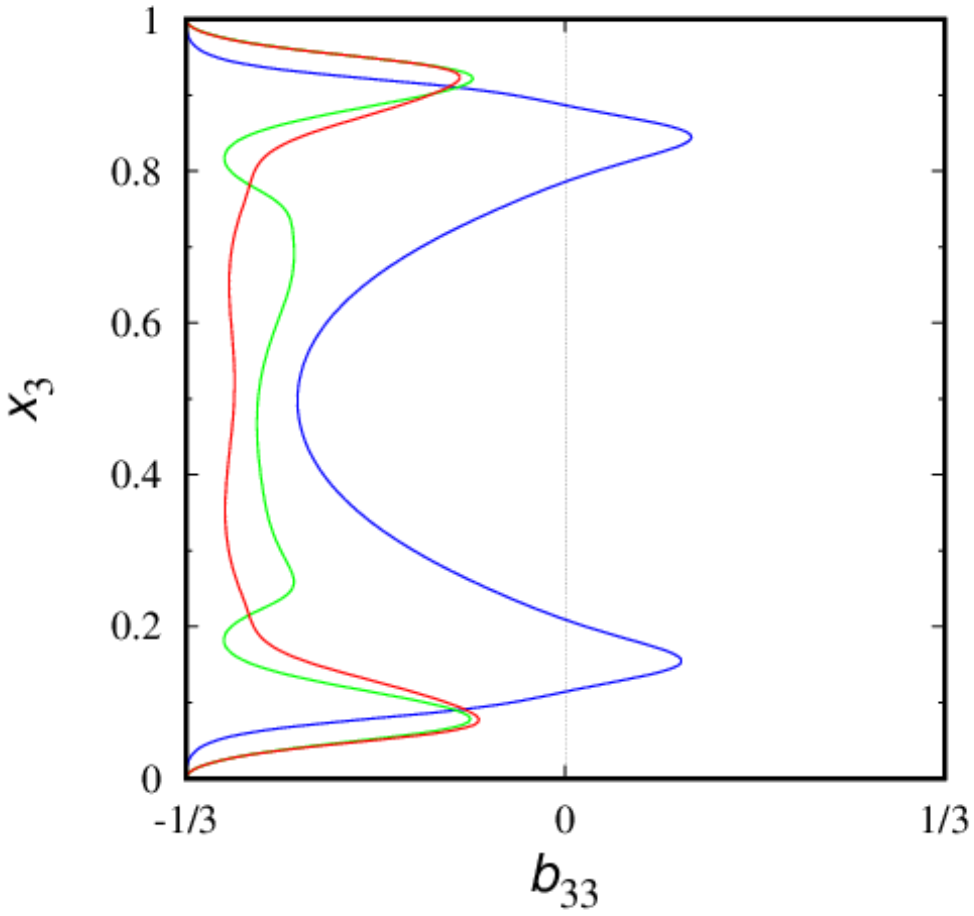

Departure-from-isotropy tensor

$$b_{ij} = \frac{\left\langle \overline{u_i' u_j'} \right\rangle}{\left\langle \overline{u_k'^{\,2}} \right\rangle} - \frac{1}{3}\delta_{ij}$$

b_{33}<0 indicates anisotropy, where the vertical-velocity fluctuations are suppressed.

The b_{33} component of the departure-from-isotropy tensor from simulations HET025 (blue), HET050 (green), and HET075 (red).

Turbulence Anisotropy, the Lumley Triangle

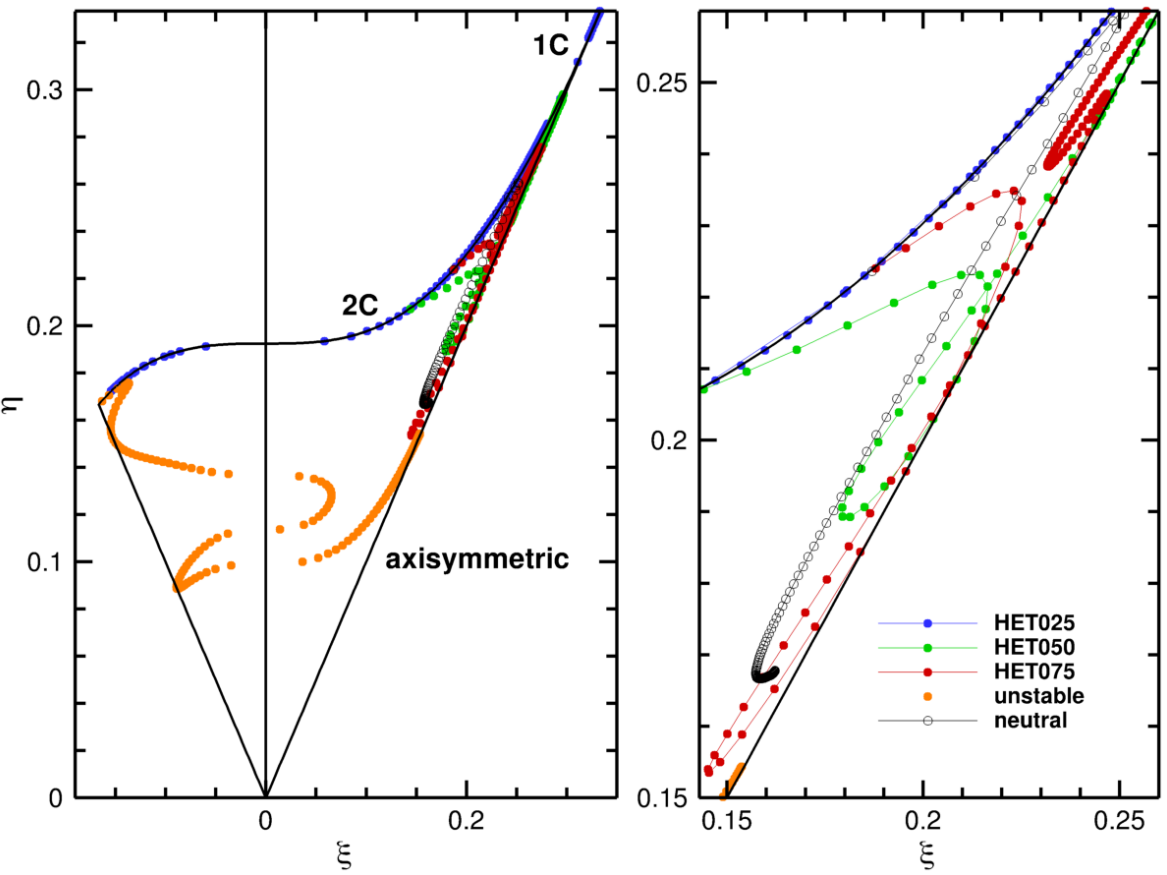

$$\frac{1}{6}\eta^2 = b_{ij}b_{ij}, \quad \frac{1}{6}\xi^3 = b_{ij}b_{jk}b_{ik}$$

$$b_{ij} = \frac{\left\langle \overline{u_i' u_j'} \right\rangle}{\left\langle \overline{u_k'^2} \right\rangle} - \frac{1}{3}\delta_{ij}$$

(**left**) The Lumley triangle on the η-ξ plane, and **(right)** a blow-up of the area close to the upper right triangle vertex corresponding to the one-component limit. Circles show data from simulations HET025 (blue), HET050 (green), and HET075 (red), and from the convective (orange) and neutrally stratified (black) Couette flows.

Temperature Variances

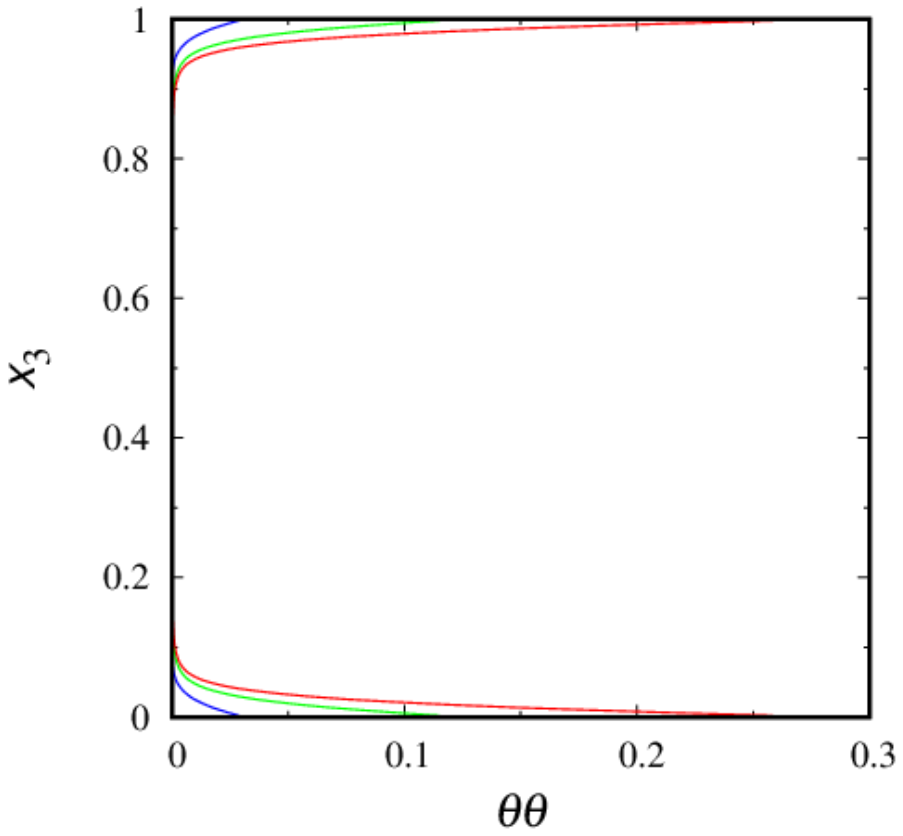

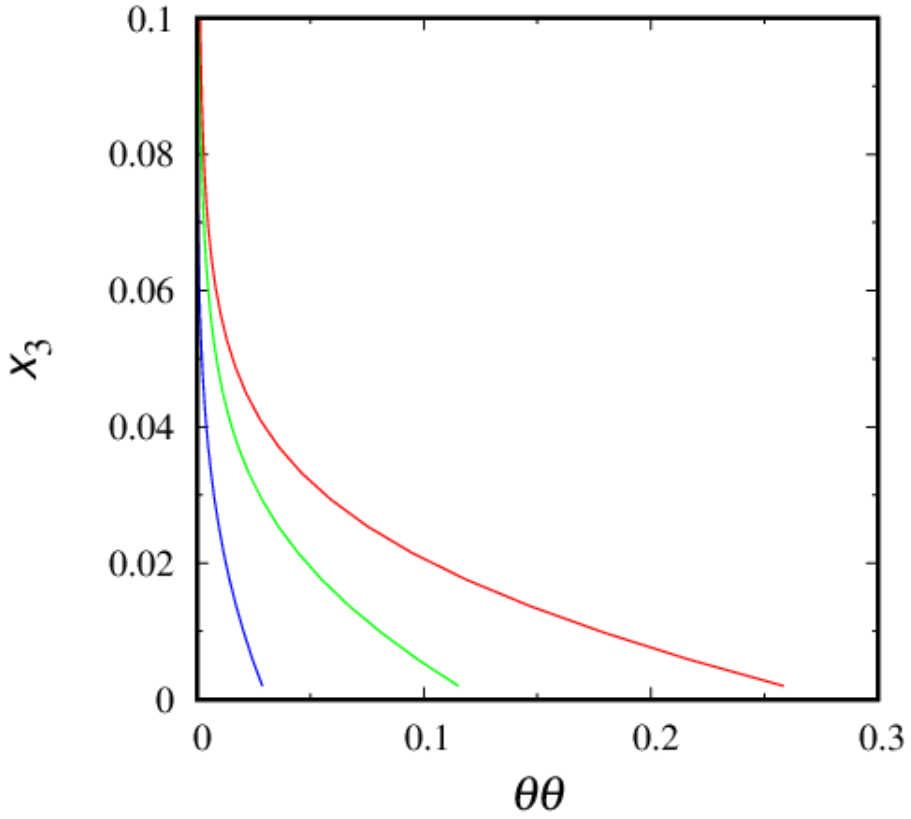

(**left**) Temperature variance from simulations HET025 (blue), HET050 (green), and HET075 (red). (**right**) The same as in the left panel but for the lower part of the domain.

Conservation of Momentum and Heat in Steady State

If the flow is stationary, the sum of vertical turbulent and molecular fluxes of streamwise momentum is depth-constant, the same holds for the vertical heat flux

$$\left\langle \overline{u_1' u_3'} \right\rangle + \frac{1}{\mathrm{Re}} \frac{\partial \left\langle \overline{u}_1 \right\rangle}{\partial x_3} = const,$$

$$\left\langle \overline{u_3' \theta'} \right\rangle + \frac{1}{\mathrm{PrRe}} \frac{\partial \left\langle \overline{\theta} \right\rangle}{\partial x_3} = const$$

Vertical Momentum Flux

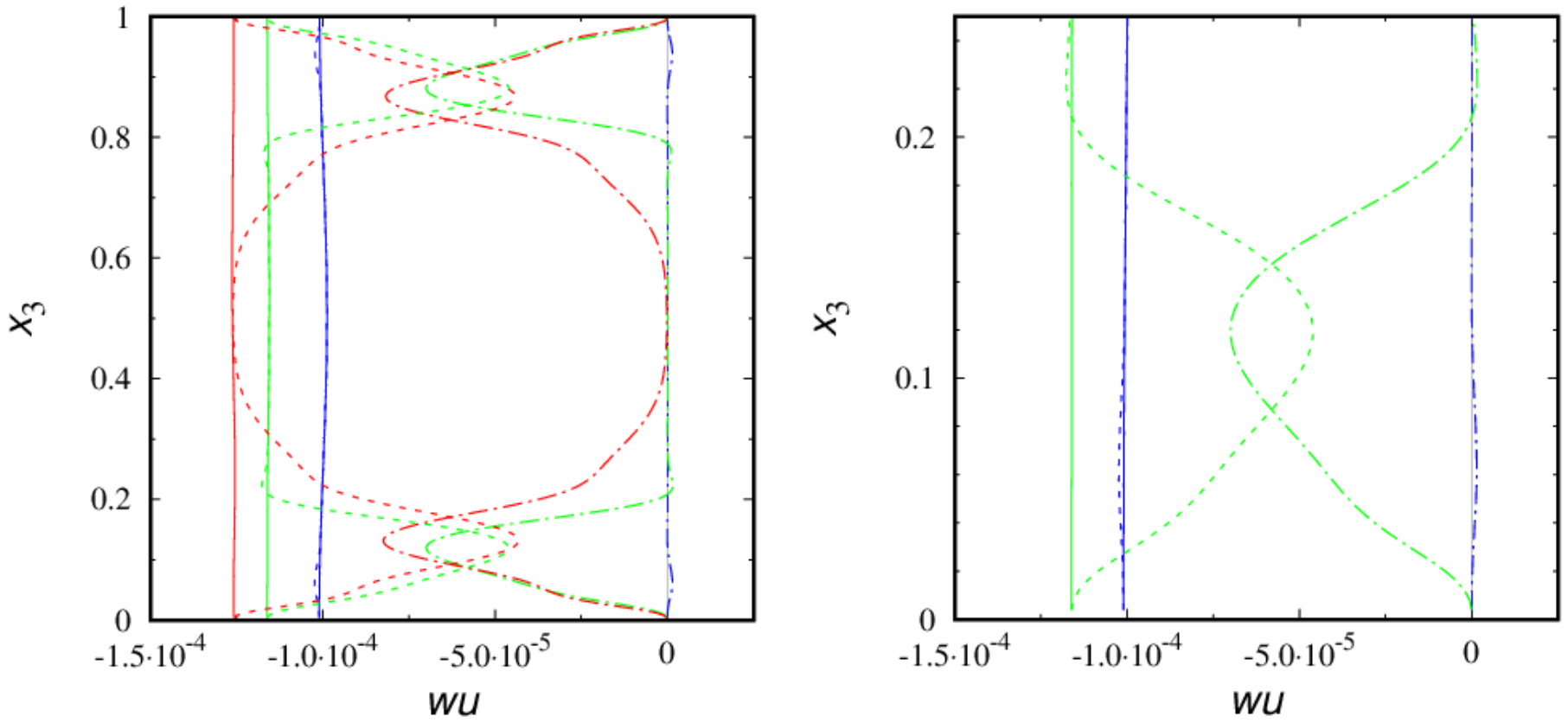

(**left**) Streamwise momentum-flux component from simulations HET025 (blue), HET050 (green), and HET075 (red). Solid curves show total (turbulent plus molecular) flux, and dot-dashed and dashed curves show contributions due to turbulence and due to molecular diffusion, respectively. (**right**) Same as in the left panel but for the lower part of the domain for simulations HET025 (blue) and HET050 (green).

Vertical Temperature Flux

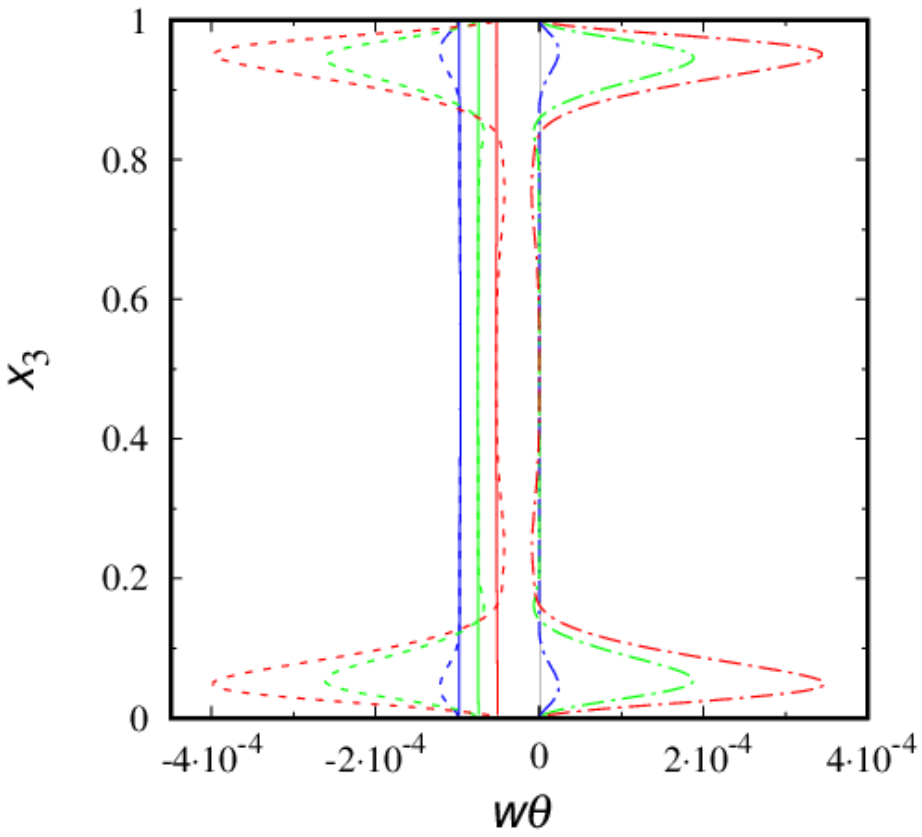

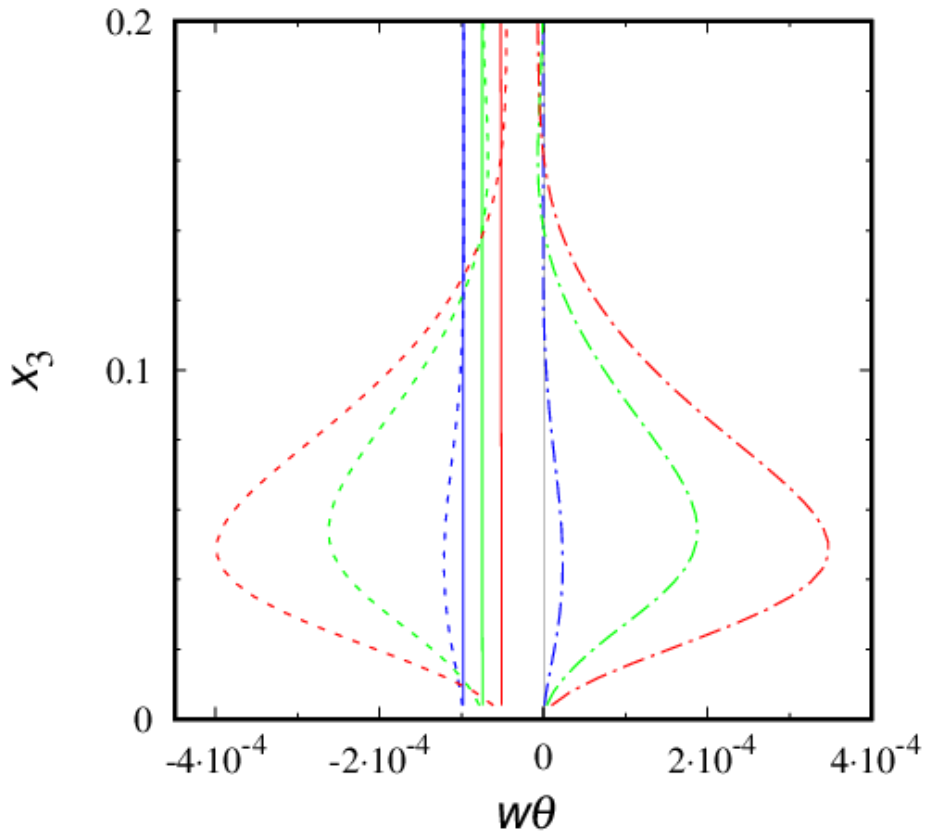

(**left**) Vertical temperature-flux component from simulations HET025 (blue), HET050 (green), and HET075 (red). Solid curves show total (turbulent plus molecular) flux, and dot-dashed and dashed curves show contributions due to turbulence and due to molecular diffusion, respectively. (**right**) The same as in the left panel but for the lower part of the domain.

Vertical-Velocity and Temperature Skewness

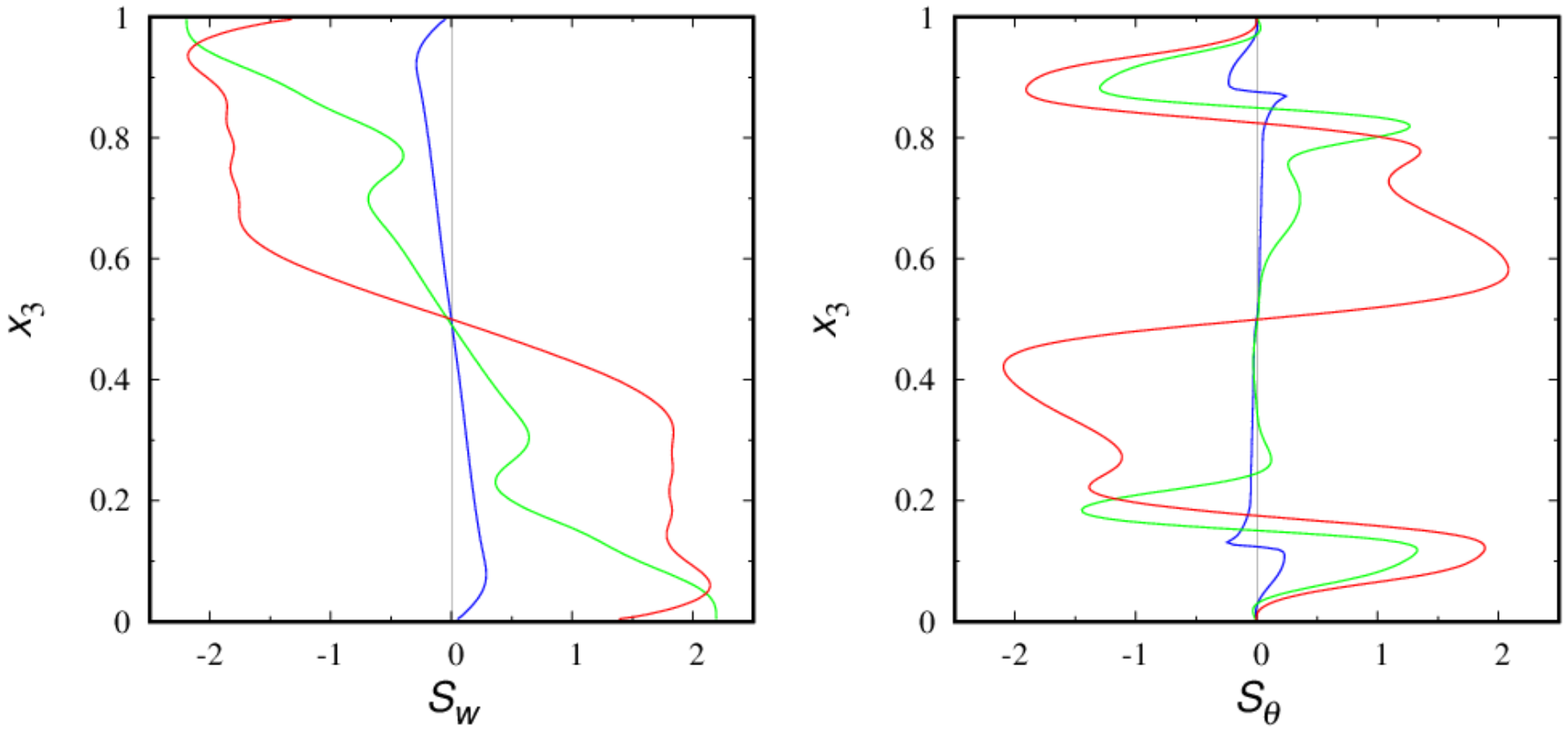

(**left**) Vertical-velocity skewness and (**right**) temperature skewness from simulations HET025 (blue), HET050 (green), and HET075 (red).

Flow Visualization

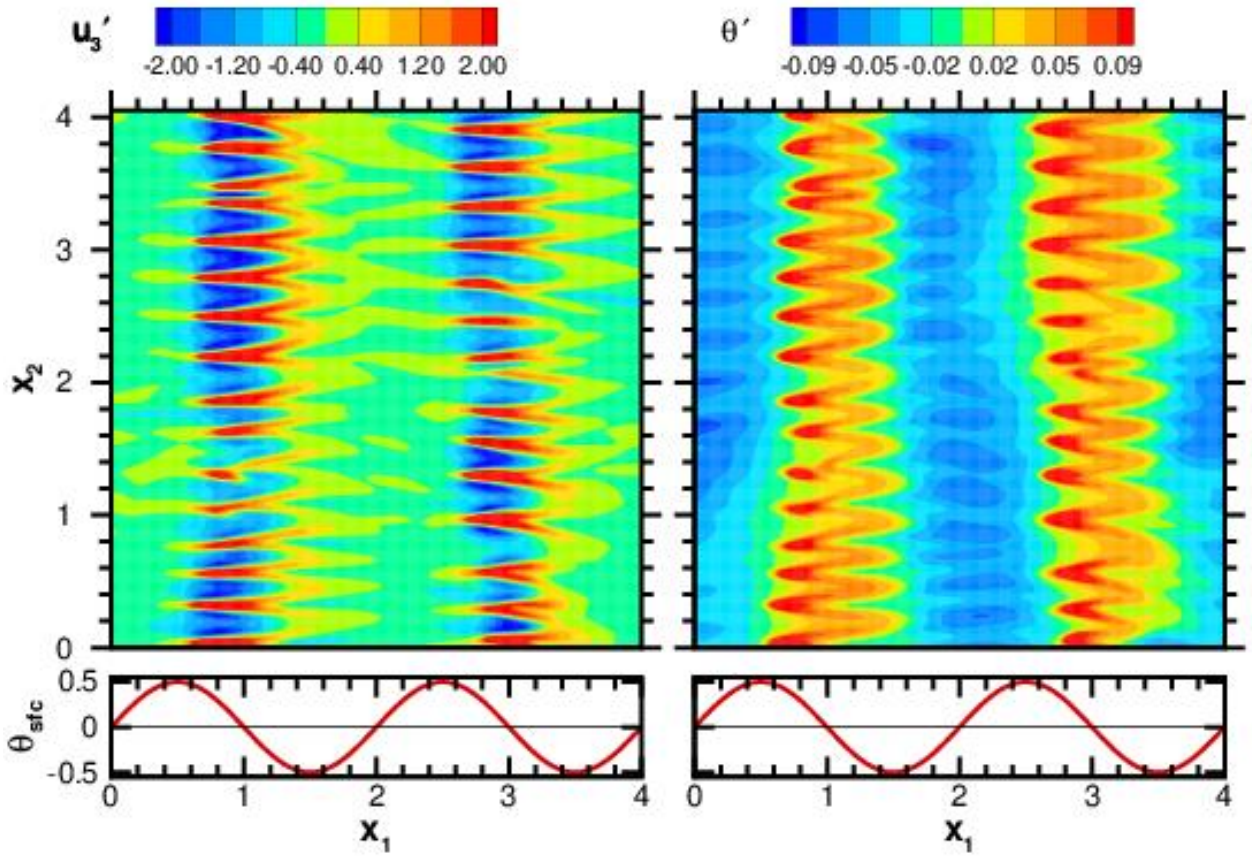

Horizontal cross sections of the fluctuations of (**left**) vertical velocity and (**right**) potential temperature about their horizontal mean values for simulation HET050. The cross section is taken at x_3= 0.076 above the lower surface near the end of the sampling period; 1/4 of numerical domain is shown. Red (blue) colors correspond to positive (negative) values of u_3' ($\times 10^2$) and θ' as shown in the color scale bars. For reference the spatial variation of the imposed surface temperature θ_{sfc} is shown in the bottom panel of each figure.

Flow Visualization (cont'd)

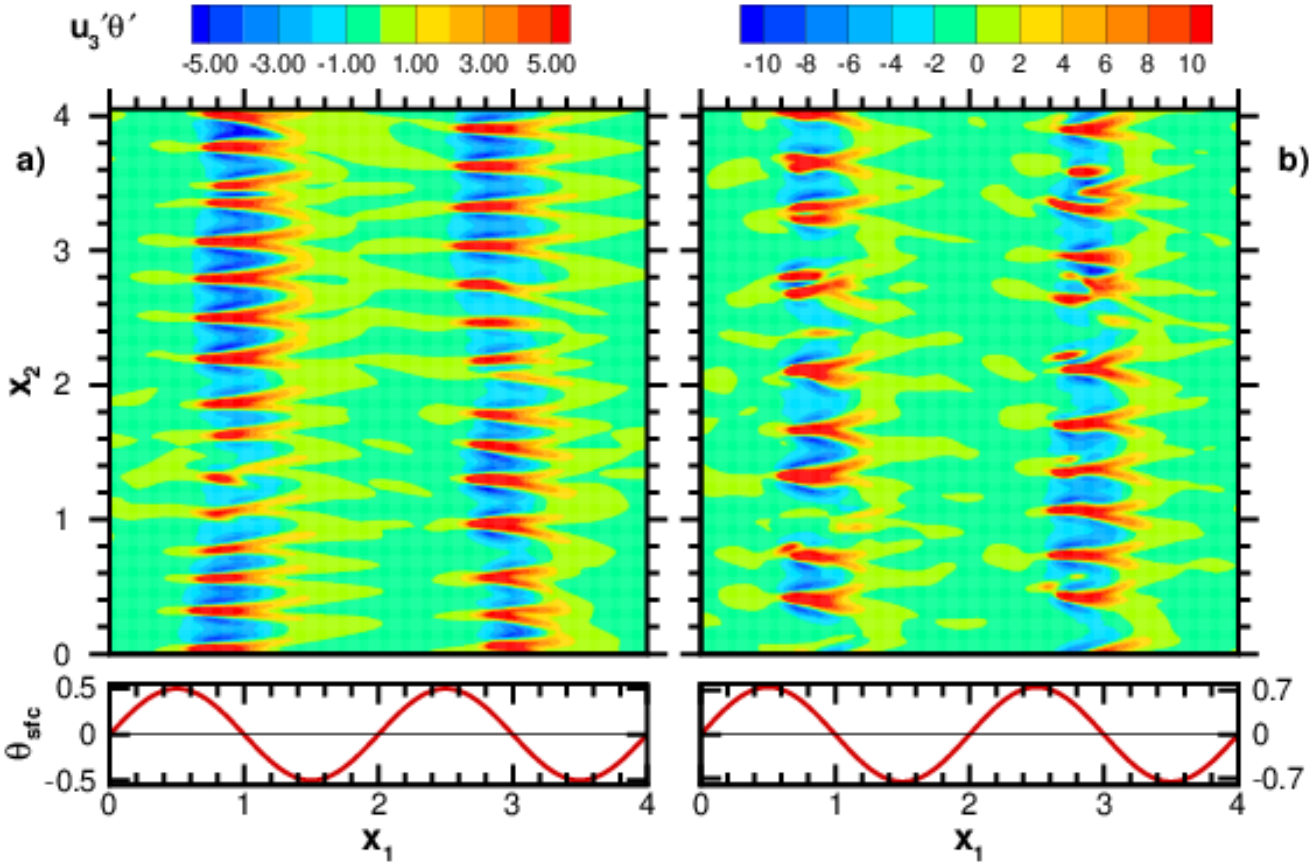

Horizontal cross sections of the resolved-scale vertical temperature flux for simulation HET050 (**left**) and HET075 (**right**). The cross sections are taken at x_3= 0.076 above the lower surface near the end of the sampling period. Red (blue) colors correspond to positive (negative) values of the temperature flux ($\times 10^3$) as shown in the color scale bar. . For reference the spatial variation of the imposed surface temperature θ_{sfc} is shown in the bottom panel of each figure.

Temperature-Variance Transport Equation

$$\frac{1}{2}\frac{\partial\langle\theta'^2\rangle}{\partial t} = -\langle u_3'\theta'\rangle\frac{\partial\langle\theta\rangle}{\partial x_3} - -\frac{1}{2}\frac{\partial\langle u_3'\theta'^2\rangle}{\partial x_3} - \varepsilon_{\theta\theta}$$

Third-order transport term
is crucial in convective flows.
In stably stratified flows,
it is typically small and can be neglected.
Then, "production=dissipation",
and turbulence model is simplified.

Importantly, $\langle u_3'\theta'^2\rangle$ is zero at the surface

if the surface is thermally homogeneous.

Third-Order Flux over Homogeneous and Heterogeneous Surfaces (LES results)

LES estimate of $\langle w'\theta'^2 \rangle$ (resolved plus SGS)

$$\left\langle \overline{\tilde{u}_3' \tilde{\theta}'^2} \right\rangle + \left\langle \overline{\tilde{u}_3' \widetilde{\theta^{s2}}'} \right\rangle + 2 \left\langle \overline{\tilde{\theta}' \widetilde{u_3^s \theta^{s}}'} \right\rangle + \left\langle \overline{\widetilde{u_3^s \theta^{s2}}} \right\rangle$$

Surface temperature variations modulate local static stability and hence the surface heat flux $\rightarrow$ net production/destruction of $\langle \theta'^2 \rangle$ due to divergence of third-order transport term!

In heterogeneous SBL, the third-order flux of temperature variance is non-zero at the surface

Third-Order Flux over Heterogeneous Surfaces

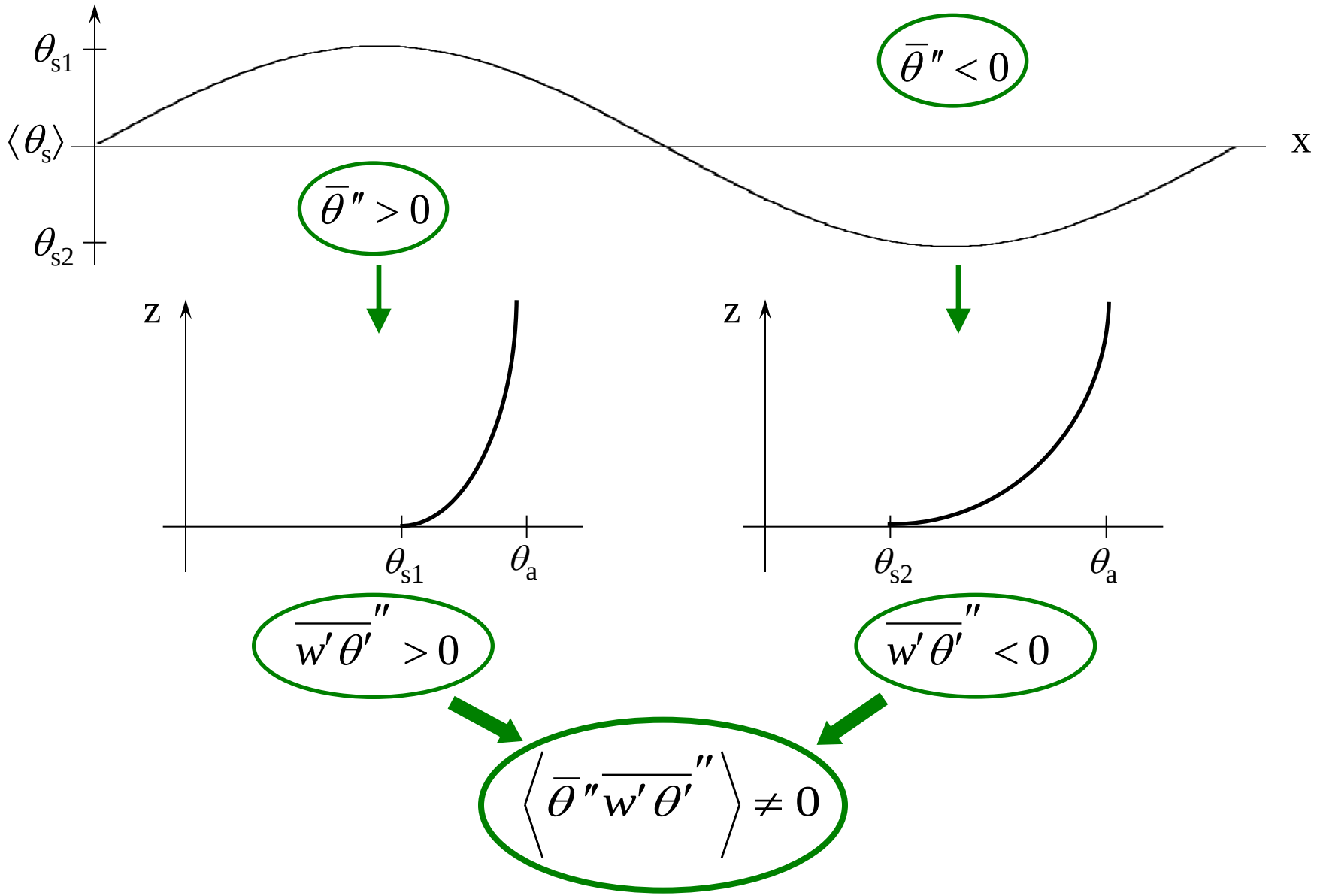

Third-Order Flux: LES vs. DNS

LES estimate of $\langle u_3'\theta'^2 \rangle$ (resolved plus SGS)

In heterogeneous SBL, the third-order flux of temperature variance is non-zero at the surface

$$\left\langle \overline{\tilde{u}_3' \tilde{\theta}'^2} \right\rangle + \left\langle \overline{\tilde{u}_3' \widetilde{\theta^{s2}}'} \right\rangle + 2 \left\langle \overline{\tilde{\theta}' \widetilde{u_3^s \theta^s}'} \right\rangle + \left\langle \overline{\widetilde{u_3^s \theta^{s2}}} \right\rangle$$

DNS estimate of $\langle u_3'\theta'^2 \rangle$

$$\left\langle \overline{u_3' \theta'^2} \right\rangle + \frac{1}{\mathrm{PrRe}} \frac{\partial \left\langle \overline{\theta'^2} \right\rangle}{\partial x_3}$$

Third-Order Flux of Temperature Variances

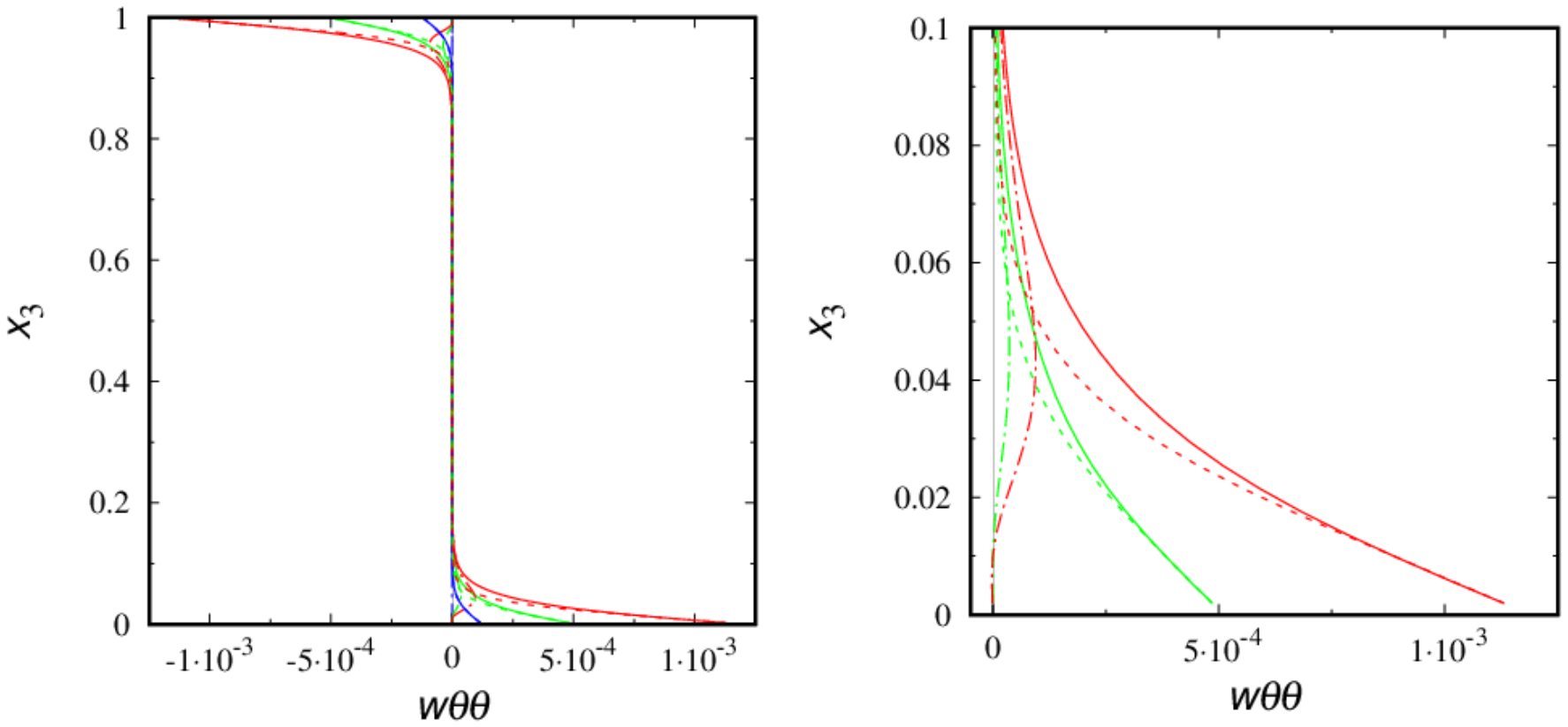

(**left**) Third-order vertical velocity-temperature covariance (vertical flux of the temperature variance) from simulations HET025 (blue), HET050 (green), and HET075 (red). Solid curves show total (turbulent plus molecular) covariance, and dot-dashed and dashed curves show contributions due to turbulence and due to molecular diffusion, respectively. (**right**) The same as in the left panel but for the lower part of the domain for simulations HET050 (green) and HET075 (red).

Implications for SBL Parameterization in Large-Scale Models (inconclusive)

$\delta\theta$ is small

- Arguably, it is not worth bothering about vertical fluxes as they are very small (though horizontal SGS motions can be of interest)

$\delta\theta$ is comparable to $\Delta\theta$ or larger

- Fluxes of momentum and scalars should be parameterized (still to be found how)
- … pragmatic tile approach may not help if stratification over all tiles is strongly stable

Work in Progress

- Analysis of second-moment budgets (TKE, temperature variance, vertical and horizontal components of temperature flux)
- Analysis of pressure-scrambling effects (pressure gradient-temperature covariance) in the temperature-flux budget, analysis of turbulence anisotropy
- Flow visualization
- HET vs. HETy

Governing Parameters of HETy Cases

In all simulated cases, **Pr=1**, **Re=10^4**, **Ri=0.25**, **n=4**, the domain size is **8**, **8** and **1**, and the number of grid points is **512**, **512** and **256**, in x_1, x_2 and x_3, directions, respectively.

Case	$\delta\theta$	T_t	T_s	$\mathbf{Re}_\tau$	$u_*\times10^2$	$Q_*\times10^5$	$1/L$
HOM	**0**	1115	15	104.63	1.05	–10.93	9.54
HET025y	**0.25**	1908	908	114.85	1.15	–9.49	6.26
HET050y	**0.50**	864	466	207.95	2.08	–20.45	2.27

Here, T_t is the total length of the simulation (in dimensionless time units), T_s is the length of the sampling period (at the end of the run), u_* is the surface friction velocity, $u_*=\mathrm{Re}^{-1}\mathrm{Re}_\tau$ is the Reynolds number based on u_*, Q_* is the surface temperature flux, and L is the Obukhov length.

In HETy cases,

temperature-wave crests are parallel to the mean flow

Flow Visualization, HET050y

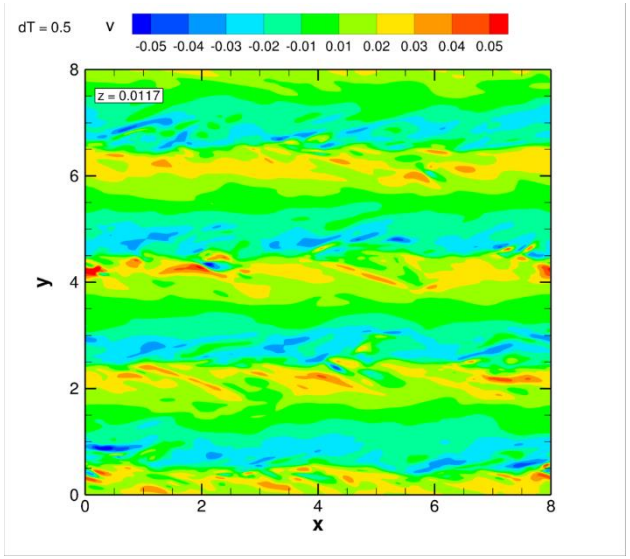

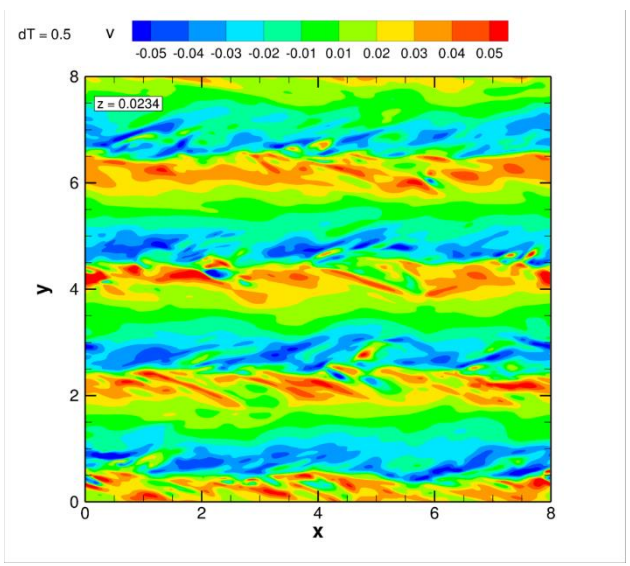

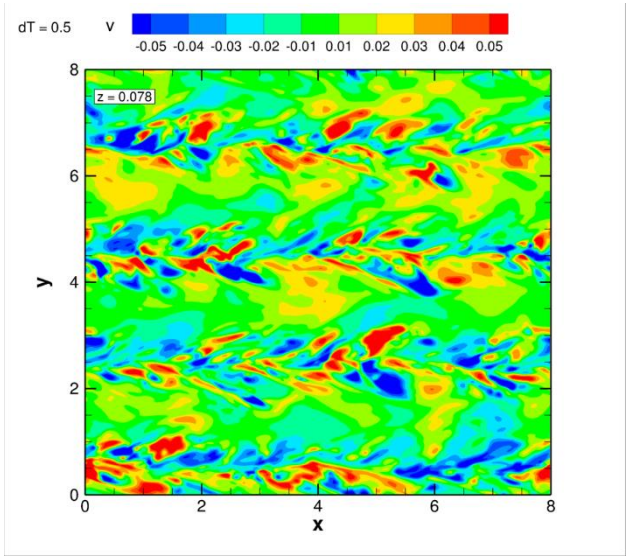

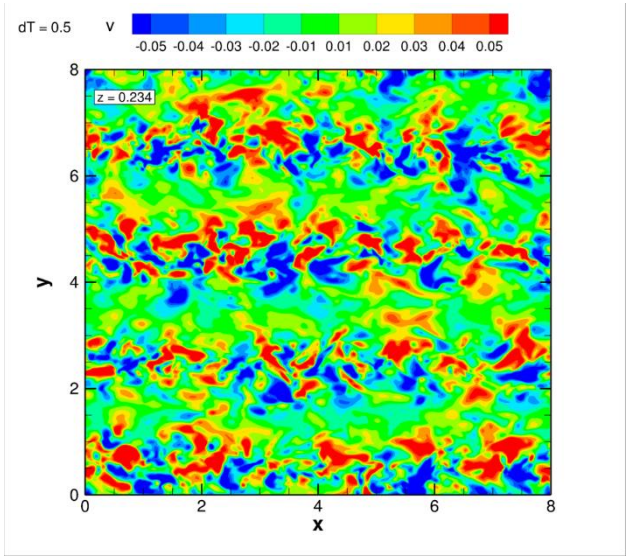

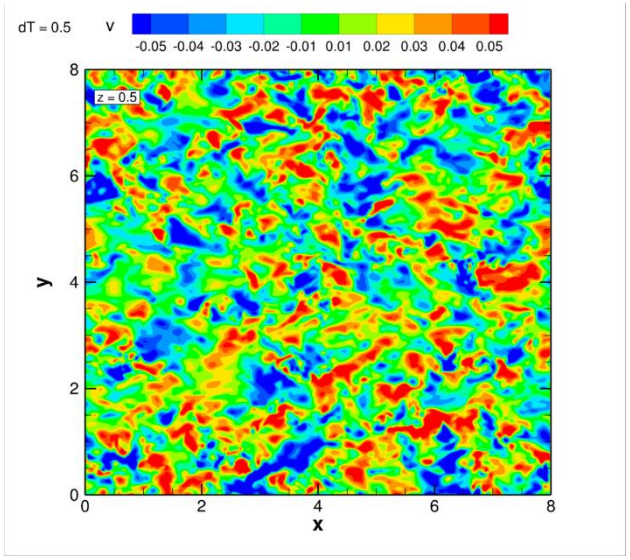

Horizontal cross sections of the spanwise velocity component at different heights above the lower surface.

HET vs. HETy: TKE

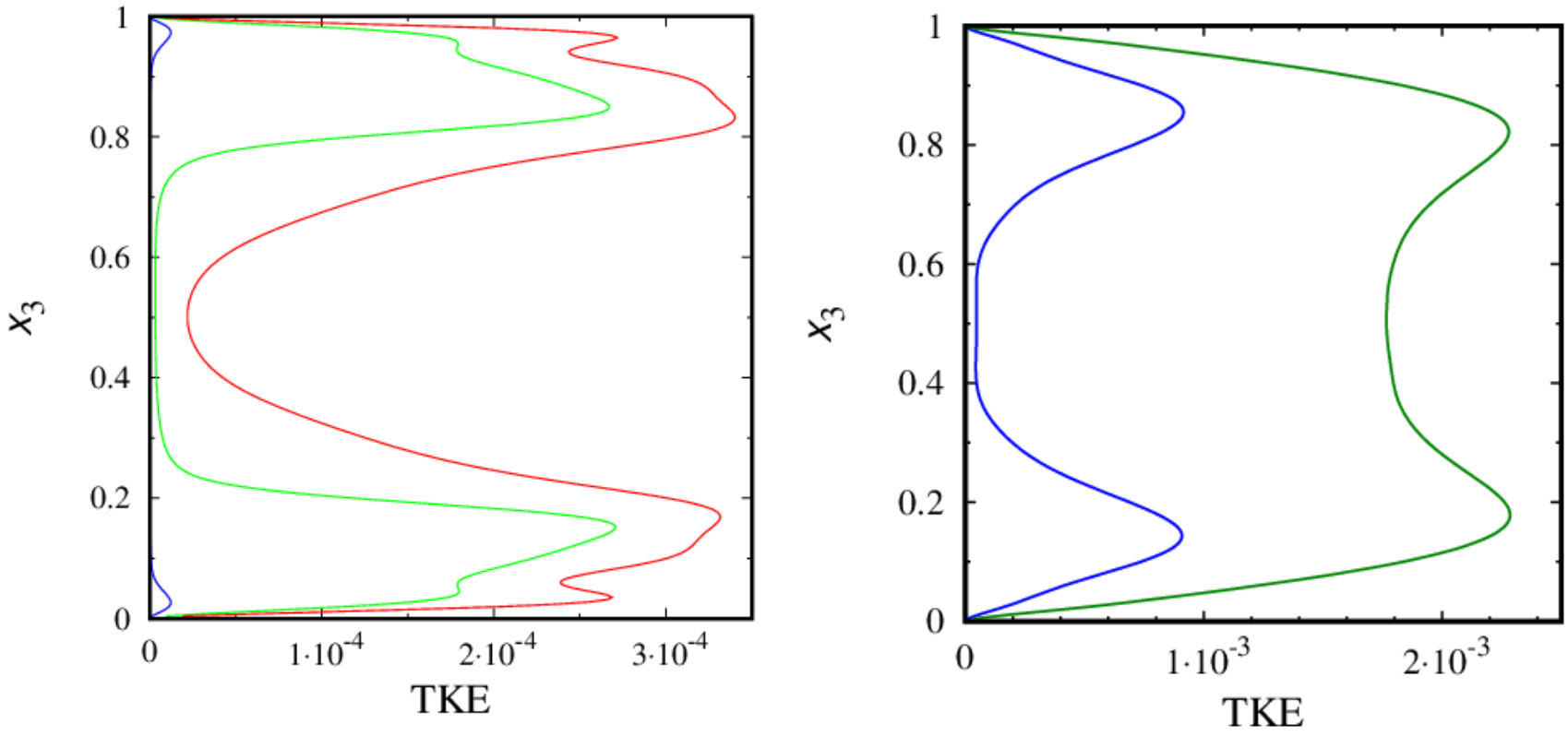

Turbulence kinetic energy from simulations (**left**) HET025 (blue), HET050 (green), and HET075 (red), and (**right**) HET025y (blue) and HET050y (green).

HET vs. HETy: Mean Temperature

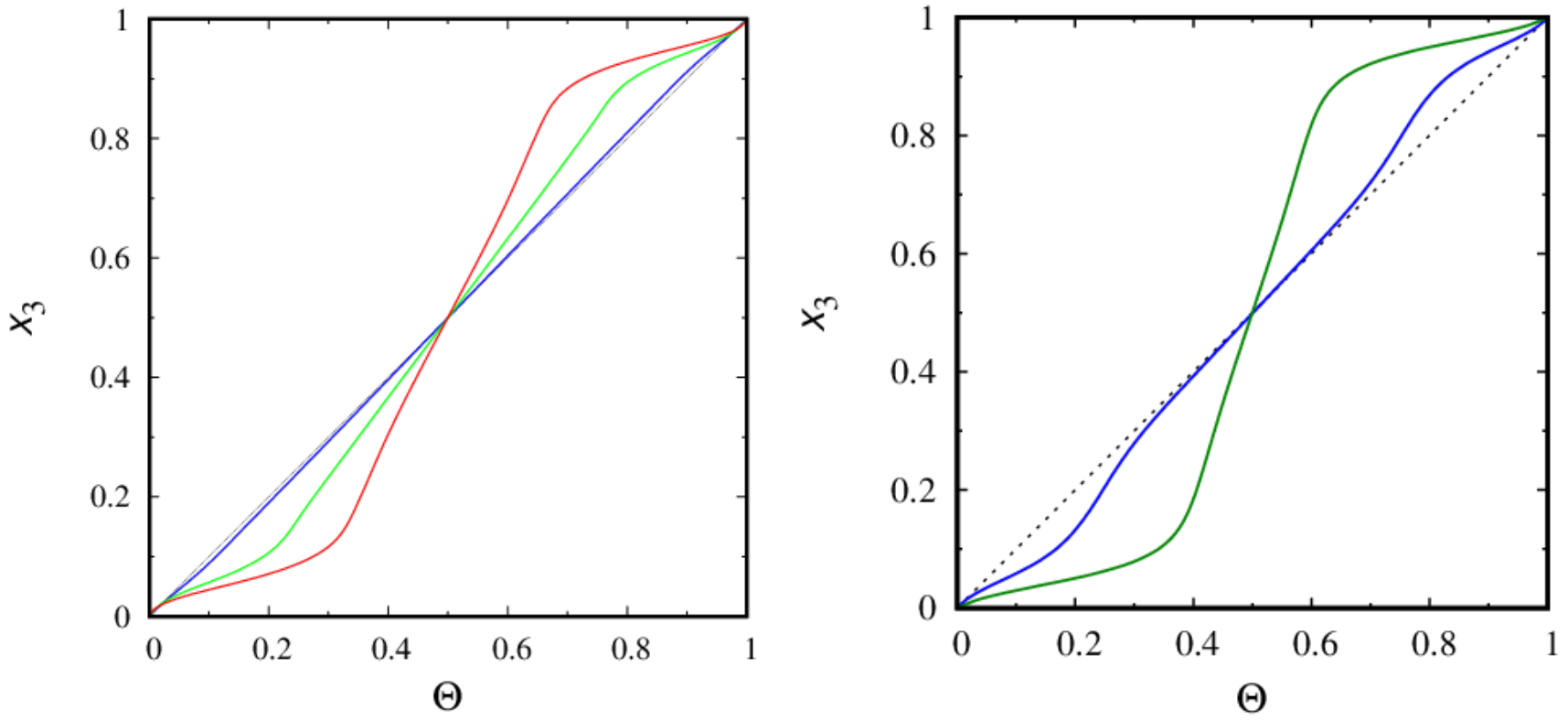

Mean temperature from simulations (**left**) HET025 (blue), HET050 (green), and HET075 (red), and (**right**) HET025y (blue) and HET050y (green).

HET vs. HETy: Mean Velocity

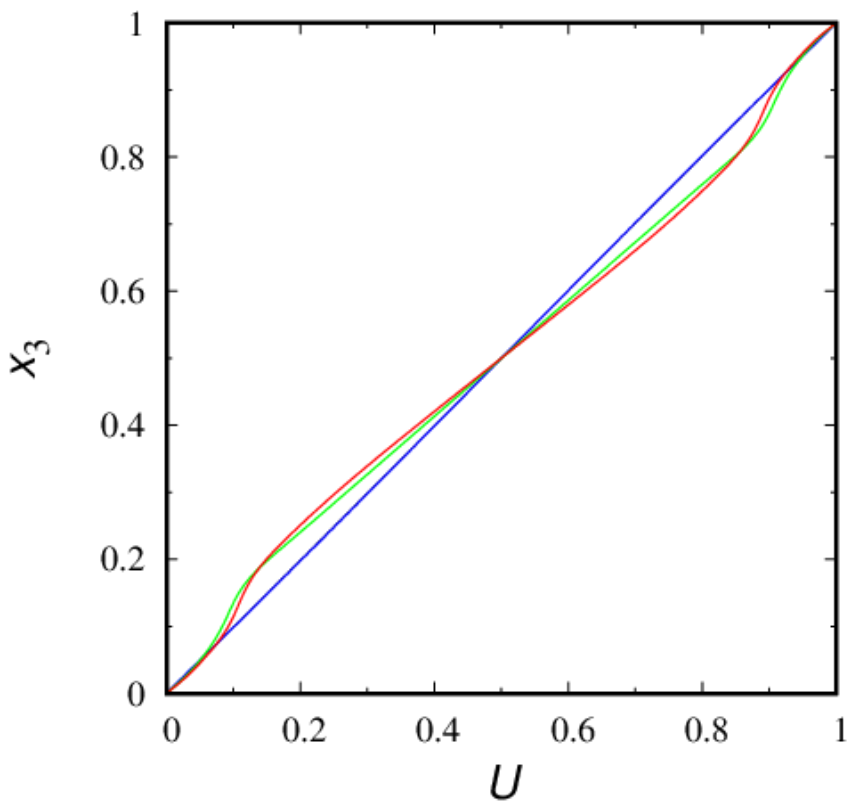

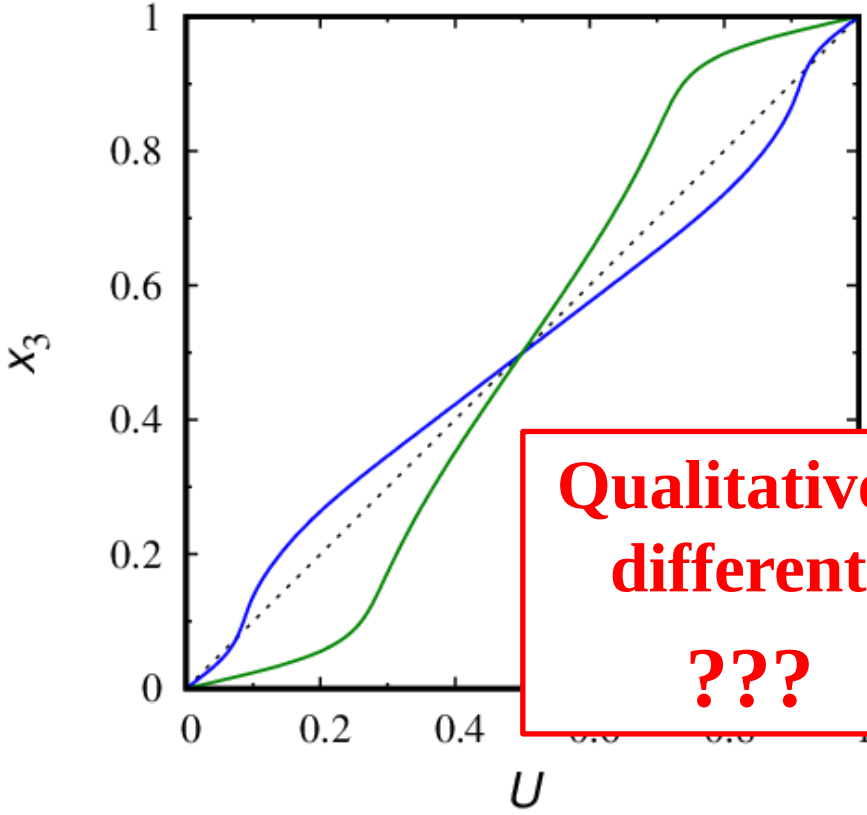

Qualitatively different!

???

Mean streamwise velocity component from simulations (**left**) HET025 (blue), HET050 (green), and HET075 (red), and (**right**) HET025y (blue) and HET050y (green).

Conclusions and Outlook

- DNS (and LES) results suggest plausible explanation of enhanced mixing in horizontally-heterogeneous SBLs
- Careful treatment of the temperature (buoyancy) variances is a key point
- Comparative analysis of HET and HETy cases (we need to solve the conundrum!)
- Perform DNS of channel and Ekman flows over heterogeneous surfaces, compare with Couette flows
- Look at real-world data (e.g., observational data on the amplitude and the spatial scales of the near-surface horizontal temperature variability vs. temperature increment across the SBL)
- Translate LES and DNS findings into parameterization ideas

References

Machulskaya, E., and D. Mironov, 2018: Boundary conditions for scalar (co)variances over heterogeneous surfaces. *Boundary-Layer Meteorol.*, **169**, 139-150. doi: 10.1007/s10546-018-0354-6

Mironov, D. V., and P. P. Sullivan, 2010: Effect of horizontal surface temperature heterogeneity on turbulent mixing in the stably stratified atmospheric boundary layer. *Proc. 19th Amer. Meteorol. Soc. Symp. on Boundary Layers and Turbulence*, Keystone, CO, USA, paper 6.3, 10 pp.

Mironov, D. V., and P. P. Sullivan, 2012: Mixing in the SBL over temperature-heterogeneous surfaces: LES findings and some parameterisation ideas. *Proc. ECMWF Workshop on Diurnal Cycles and the Stable Boundary Layer*, European Centre for Medium-Range Weather Forecasts, Reading, UK, 149-151.

Mironov, D. V., and P. P. Sullivan, 2016: Second-moment budgets and mixing intensity in the stably stratified atmospheric boundary layer over thermally heterogeneous surfaces. *J. Atmos. Sci.*, **73**, 449-464. doi: 10.1175/JAS-D-15-0075.1

Mironov, D., and P. Sullivan, 2018: Turbulence Structure and mixing in strongly stable boundary-layer flows over thermally heterogeneous surfaces. *Proc. 23rd Amer. Meteorol. Soc. Symp. on Boundary Layers and Turbulence*, Oklahoma City, OK, USA, paper 1B.3, 12 pp.

Mironov, D. V., and P. P. Sullivan, 2021: Effect of surface thermal heterogeneity on the structure and mixing intensity in strongly stable boundary-layer flows: a DNS study. *10th International Symposium on Turbulence, Heat and Mass Transfer*, St. Petersburg, Russia. 4 pp.

Sullivan, P. P., J. C. Weil, E. G. Patton, H. J. J. Jonker, and D. V. Mironov, 2016: Temperature fronts and vortical structures in turbulent stably stratified atmospheric boundary layers. *Proc. VIIIth International Symposium on Stratified Flows*, San Diego, CA, USA, 8 pp.

Sullivan, P. P., J. C. Weil, E. G. Patton, H. J. J. Jonker, and D. V. Mironov, 2016: Impacts of surface cooling on turbulence and temperature fronts in the stable atmospheric boundary layer. *22nd Amer. Meteorol. Soc. Symp. on Boundary Layers and Turbulence*, Salt Lake City, UT, USA.

Sullivan, P. P., J. C. Weil, E. G. Patton, H. J. J. Jonker, and D. V. Mironov, 2016: Turbulent winds and temperature fronts in large-eddy simulations of the stable atmospheric boundary layer. *J. Atmos. Sci.*, **73**, 1815-1840. doi: 10.1175/JAS-D-15-0339.1

Sullivan, P. P., and D. V. Mironov, 2022: Turbulence structure and mixing in strongly stable boundary-layer flows over thermally heterogeneous surfaces. Submitted to *Boundary-Layer Meteorol.*

Thank you for your kind attention!

Acknowledgements: Thanks are due to Vittorio Canuto, Sergey Danilov, Alberto de Lozar, Evgeni Fedorovich, Vladimir Gryanik, Jürgen Helmert, Donald Lenschow, Juan Pedro Mellado, Chin-Hoh Moeng, Ned Patton, Matthias Raschendorfer, Chiel van Heerwaarden, and Jeffrey Weil for discussions. The work was partially supported by the NCAR Geophysical Turbulence Program and by the European Commission through the COST Action ES0905. NCAR is sponsored by the National Science Foundation.